

Connectivity Patterns of Interictal Epileptiform Discharges Using Coherence Analysis

Panuwat Janwattanapong¹, Mercedes Cabrerizo¹, Alberto Pinzon², Sergio Gonzalez-Arias^{2,3}, Armando Barreto¹, Jean Andrian¹, and Malek Adjouadi¹

¹Center for Advanced Technology and Education, Department of Electrical and Computer Engineering Florida International University (FIU)

²Baptist Health Neuroscience Center, Baptist Hospital of Miami

³ FIU Herbert Wertheim College of Medicine

Abstract— this paper introduces the patterns generated from the functional connectivity extracted from electroencephalogram (EEG) by implementing the coherence analysis. Three types of epileptiform discharges (interictal spike, spike and slow wave complex, and repetitive spikes and slow wave complex) are classified by the quantification of functional connections presented in the regions of interest within different frequency bands (Delta, Theta, Alpha, and Beta). These patterns are validated by performing analysis of variance (ANOVA). Results revealed that the number of connections from different epileptogenic biomarkers were statistically different. The functional connectivity maps were able to delineate the distinctive patterns that can be used to classify different types of epilepsy.

Keywords— *Interictal EEG; Functional Connectivity; Coherence analysis; Pattern classification; Frequency band*

I. INTRODUCTION

Epilepsy is a chronic disorder and is one of the most common neurological disorders affecting approximately 0.5 – 1 % of the entire population. The major characteristic which defines the disorder is the recurrent unprovoked seizures. In the period of seizures, groups of neurons located in the cerebral cortex are being uncontrolled and excessively triggered at the same time resulting in symptoms such as muscle spasms and impaired consciousness [1]. Although the symptoms mentioned above are general symptoms, the location of event, duration of seizure or how the seizure propagates vary depending on the individual. Due to the unpredictable occurrence of seizures, the quality of life of epileptic patients might be greatly impacted by this uncertainty. Therefore enhancing epilepsy diagnosis or even predict the occurrence of seizure through the electroencephalogram (EEG) recordings could lead to better planning and therapeutic protocols, which will definitely benefit epileptic patients and society at large especially when evaluating EEG recording is the most common epilepsy diagnostics.

Among the neurophysiological techniques, EEG still remains the most prevalent modality to examine brain activities as well as using it as the main diagnosis assessment

[2]. EEG captures the electrical activities produced by the neurons in the brain including the epileptiform discharges (ED). Due to its high temporal resolution, EEG is considered a suitable tool for identifying synchronization between a pair of signals [3], which makes EEG an important tool to extract the functional connectivity.

The study of functional connectivity has received great attention in the field of neuroscience and has yielded promising results in diverse research endeavors [2, 4, 5, 6, and 7]. Functional connectivity is defined as a study of the correlation of event occurring in the regions of the cortex [8]. The value of functional connectivity depends on the levels of synchronization between groups of neurons, which can be estimated from EEG recordings by using one of the most promising measures such as coherence measurement [9]. EEG coherence provides the interactions between neural activities in different frequencies across brain regions, which in this case, it will be used to analyze the pattern of ED where it is perceived that the characteristics of different types of epileptiform discharges will be distinct from each other creating a pattern that will be used as classification parameters.

This study proposes an analysis of functional connectivity patterns extracted from the EEG data containing ED by using coherence method in each of the frequency bands (Delta, Theta, Alpha, and Beta). EEG contains a specific clinical and physiological range of frequency components of interest, which is between 0.3 – 30 Hz, where frequency components higher than 30 Hz (Gamma) are usually found not to be related to epileptiform discharges [10]. In this paper we want to limit the search to this frequency range since scalp EEG data is usually manually screened using a band pass filter with cut-off frequencies from 0.5 to 35Hz. Coherence of all the pair-wise electrodes are calculated creating connectivity matrices base on the placement of the electrodes. High value of coherence indicates the strong connection between the selected pair of electrodes and low values infer otherwise. After thresholds are applied, the connectivity matrices are quantified and validated by performing analysis of variance (ANOVA) to generate patterns of each type of EDs.

II. MATERIAL AND METHODOLOGY

The overall structure of the algorithm, together with its main steps, is shown as a flow diagram in Fig. 1. After the

Research is supported by the National Science Foundation under grants CNS 1532061, CNS-0959985, HRD-0833093, CNS-1042341, CNS-1551221, and IIP-1338922. Support of the Ware Foundation is also greatly appreciated.

functional connectivity extraction, the number of connections in the regions of interest (ROI) was collected. A statistical analysis was applied to analyze the pattern of different type of EDs.

A. Data acquisition

In this study only epileptiform discharges were used to extract the different characteristics of the 3 types of epileptic biomarkers, which are: (a) interictal spike (b) spike with slow wave complex (c) repetitive spikes and slow wave complex. In order to explore synchronization between brain regions in focal and generalized cases, a total of 30 EEG segments from a male patient diagnosed with generalized epilepsy and a female patient diagnosed with focal epilepsy having partial complex seizures were obtained. The data were recorded with the 10-20 electrode placement protocol containing 3 types of epileptiform discharges (ED), namely interictal spike (IS), spike and slow wave complex (SSC), and repetitive spikes and slow wave complex (RSS). Recordings are performed containing 19 electrodes (Fp1, F7, T3, T5, O1, F3, C3, P3, Fz, Cz, Pz, Fp2, F8, T4, T6, O2, F4, C4, and P4) using referential montage. The data was collected with a sampling rate of 200 Hz.

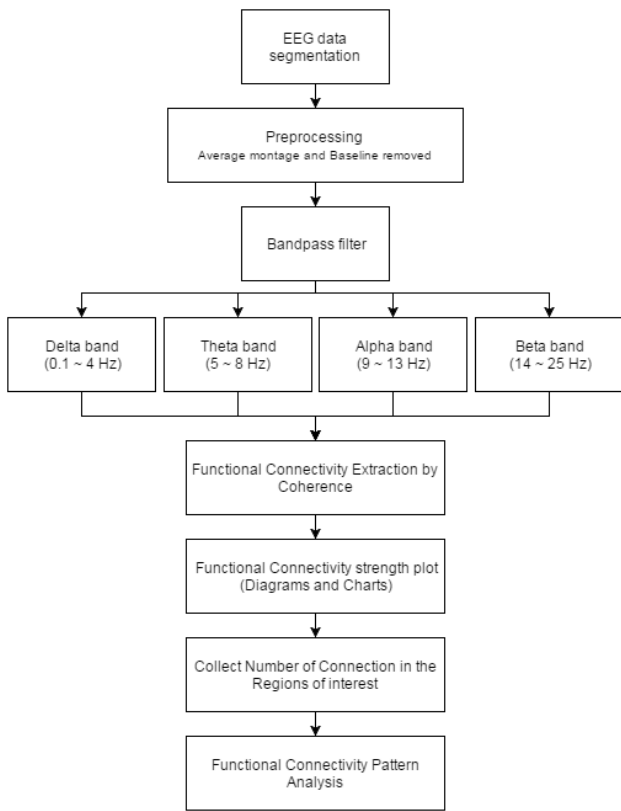


Fig. 1. Flow diagram of the process

B. Preprocessing

The EEG data was divided into 3 separated groups according to the types of EDs. They were segmented into 1-second window containing a single occurrence of ED in the

center of the segment. EDs of IS were arranged at the 0.5 s of the segment, where SSC and RSS were arranged at the 0.2 s of the segment due to its longer extent. In total, 10 segments of each type of EDs were extracted from the original EEG data.

The data was converted from a referential montage to an average montage in order to reduce the effect of volume conduction [11]. A zero-phase finite impulse response (FIR) bandpass filter (0.1 – 30 Hz) from EEGLAB [12] was implemented to filter the frequency bands of interest and to remove the artifacts. The focus was placed on the four following frequency bands, Delta band [0.1 - 4 Hz], Theta band [5 – 8 Hz], Alpha band [9 – 13 Hz], and Beta band [14 – 25 Hz].

C. Functional Connectivity with Coherence

Functional connectivity was extracted by performing a computation of coherence between all pairwise 19 multichannel EEG electrodes. Coherence between two signals $x(t)$ and $y(t)$, which in this case, $x(t)$ and $y(t)$ represent a vector of the data of an electrode measurement with each containing 200 data points, is defined as the magnitude squared of the cross-spectral density between 2 designated signals divided by the product of power spectral densities (PSD) of each of the signals as shown in (1) where f is the selected frequency.

$$C_{xy}(f) = \frac{|G_{xy}(f)|^2}{G_{xx}(f)G_{yy}(f)} \quad (1)$$

$G_{xx}(f)$ and $G_{yy}(f)$ denotes the calculated PSD of signal x and y respectively and $G_{xy}(f)$ represents the cross-spectral density of signal x and y . In this methodology, Welch's average periodogram [12] has been implemented to calculate the coherence. The method computes the modified periodogram for the segments and averages the output to estimate the PSD of the time series. In this research, 0.5s hamming windows with 50% overlap had been used to calculate the PSD of the 1s epoch, where the overlap protects the loss of information caused by windowing. The results obtained from this method provided a better performance compared to other estimation algorithm [4] in terms of signal to noise ratio. The computed coherences were then examined within the frequency bands of interest by obtaining the average coherence value for each of the 4 frequency bands as shown in (2)

$$A_{xy}(f) = \frac{\int_L^U c_{xy}(f) df}{U-L} \quad (2)$$

U is the upper bound and L is the lower bound of the selected frequency. For example, if the Delta band is selected, the lower bound and the upper bound that will be used are [0.1, 4 Hz] respectively. The computed average coherence coefficients vary in a range of 0 to 1, where 0 indicates that there is no connection between the pair of electrodes where 1 indicates that there is a strong connection. The values of average coherence extracted from each pair of electrodes together form a matrix called connectivity matrix. After the connectivity matrices for every frequency band of interest and

each type of EDs were obtained, the connectivity matrices were then applied with different thresholds (50%, 70%, 80%, 90%, and 95%). The head map connectivity plots, which are shown in the results section, were analyzed and validated by statistical tests.

D. Quantification of Functional Connectivity

The brain cortex was subdivided into different regions based on two specific cases. The subdivision of the first case was done by dividing the cortex based on the left and right hemispheres (LR region). The activities on the left hemispheric region included Fp1, F7, T3, T5, O1, F3, C3, and P3 electrodes and the right hemispheric region contained Fp2, F8, T4, T6, O2, F4, C4, and P4 electrodes. The LR region was separated by the central line, which is a longitudinal fissure that contains Fz, Cz, and Pz electrodes. Connections between a pair of electrodes occurring within the right hemispheric region were labeled as the “right intra-connection”. The same concept was applied to the left hemispheric region as well, where the labeled connection was identified as “left intra-connection”. If the connection occurs between the two hemispheres, the connection was labeled as “LR interconnection”.

The subdivision of the second case was done base on the anterior-posterior regions (AP region), where the anterior region contained Fp1, Fp2, F7, F3, Fz, F4, and F8 electrodes and the posterior region contained T5, P3, Pz, P4, T6, O1, and O2 electrodes. These regions were separated by the electrodes located along the central sulcus line, which contains T3, C3, Cz, C4, and T4 electrodes. The same principle of identifying these connections were applied to this case with the labels “anterior intra-connection”, “posterior-intra-connection”, and “AP interconnection”.

Fig. 2 illustrates the specified regions of interest that was used in the quantification process. The number of connections obtained was used as one of the features to be analyzed using variance (ANOVA) statistical test. Each type of EDs are expected to carry different characteristics which varies in different frequency bands and thresholds used.

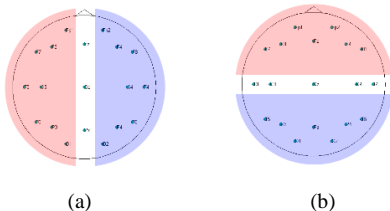


Fig. 2. Regions of interest, group (a) left-right hemisphere (Left – red, Right – blue) (b) anterior-posterior axis (Anterior – red, Posterior – blue).

III. RESULTS

The connectivity results from the feature extraction are displayed separately by the specific frequency bands. The head map average connectivity plots were obtained by taking an average of the connectivity matrices from the extracted 10 segments. The color indicates the strength of the connection,

where dark red indicates strong connections and dark blue indicates weaker connections.

A. Delta Band

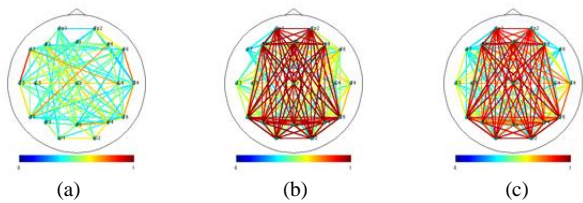


Fig. 3. Head map average connectivity plots for (a) interictal spike (b) spike with slow wave complex (c) repetitive spikes and slow wave complex from Delta Band

The results of the head map average connectivity plots of the Delta frequency band shown in Fig. 3 reveal some differences in the number and strength of connections between each type of ED. The connectivity map of IS shows a significantly less propagation between AP and LR regions and the strong connection is displayed only in the temporal lobe region between F7 and T3 electrodes. The observation obtained infers that these characteristic are related to focal epilepsy. On the contrary, the connections of SSC and RSS propagate throughout the entire cortex including AP and LR regions with very strong connections, inferring that these features fall into a generalized type of epilepsy.

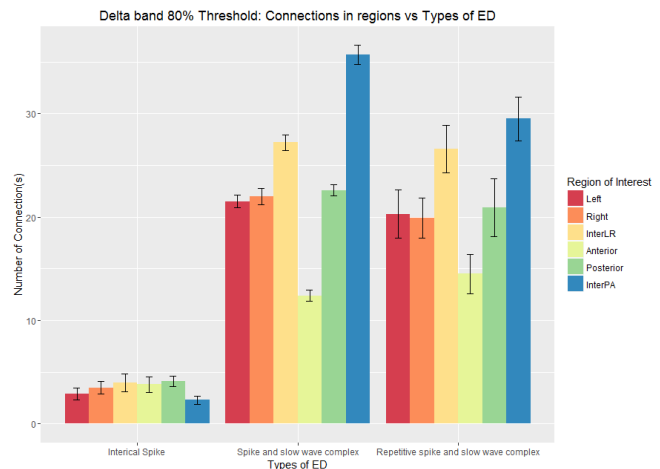


Fig. 4. Mean and standard deviation with 80% threshold in the Delta band

Fig. 4 shows the mean and standard deviation of the strongest connections (Average coherence value greater than 0.80) for each type of EDs in the different ROIs within the Delta band. The ANOVA was calculated for each type of EDs with the null hypothesis that, the number of strong connections of the different ROIs is the same within each type of EDs. The analysis for IS type is not significant with ($F(5, 54) = 1.2142$, $p\text{-value} > 0.31$), resulting in accepting the null hypothesis; whereas the analyses for SSC and RSS are significant with ($F(5, 54) = 114.98$, $p\text{-value} < 0.00$) and ($F(5, 54) = 5.6458$, $p\text{-value} < 0.00$) respectively. By analyzing 3

different types of ED, it was noted that the number of stronger connections of SSC and RSS differed from IS significantly with ($F(2,177) = 175.13$, p-value < 0.00), whereas the post-hoc analysis indicated that the ED types with the highest number of stronger connections are SSC and RSS respectively.

B. Theta Band

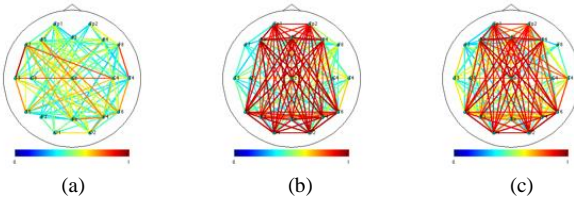


Fig. 5. Head map average connectivity plots for (a) interictal spike (b) spike with slow wave complex (c) repetitive spike and slow wave complex in the Theta Band

The obtained average connectivity head map plots in Theta band shown in Fig. 5 illustrate similar result as Delta band. The IS stronger connections between LR region increased when compared to the previous frequency band, but in general, the pattern of IS still shows characteristics presented in a focal epileptic behavior.

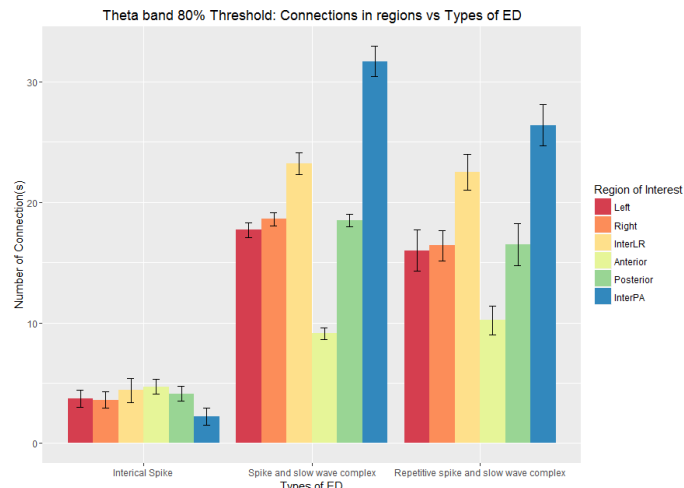


Fig. 6. Mean and standard deviation with 80% threshold in Theta band

The mean and standard deviations of the strongest connections in Theta band, as shown in Fig. 6 has been applied by the same statistical analysis under the same null hypothesis. The calculated ANOVA for IS type is not significant with ($F(5, 54) = 1.4633$, p-value > 0.21), whereas the analyses for SSC and RSS are significant with ($F(5, 54) = 94.175$, p-value < 0.00) and ($F(5, 54) = 13.588$, p-value < 0.00) respectively. The results reveal the same characteristics and patterns found in the Delta band. The numbers of the strongest connections for each ROI for IS type are not statistically different, which varied from SSC and RSS with (F

(2, 177) = 130.35, p-value < 0.00) that rejects the null hypothesis.

C. Alpha Band

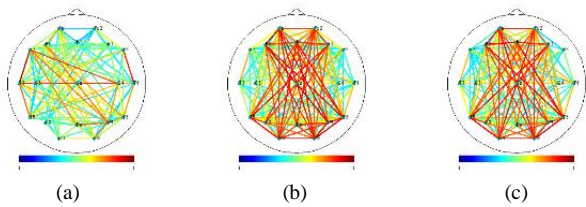


Fig. 7. Head map average connectivity plots for (a) interictal spike (b) spike with slow wave complex (c) repetitive spike and slow wave complex from Alpha Band

The strongest connections obtained in Alpha band from SSC and RSS showed a decrease in the propagation when compared to Delta and Theta band results, whereas the activities obtained for IS are not significant different from the previous frequency bands outcome. By comparing within Alpha band, SSC and RSS still provide a higher propagation, which indicate the generalized type of epilepsy.

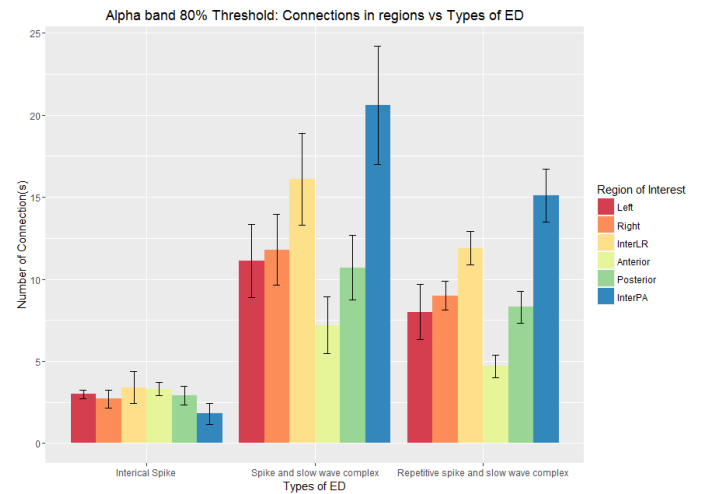


Fig. 8. Mean and standard deviation with 80% threshold in Alpha band

Same statistical analysis has been applied to the mean and standard deviation of the Alpha band results shown in Fig. 8. Similar results were obtained from the calculations. The difference is not significant, whereas the null hypothesis for IS type was accepted with ($F(5, 54) = 0.897$, p-value > 0.48). The analyses for SSC and RSS still exhibited similar results with the rejection of the null hypotheses, ($F(5, 54) = 3.561$, p-value < 0.00) and ($F(5, 54) = 8.9211$, p-value < 0.00). SSC and RSS also contained a significant amount of stronger connections when compared to IS.

D. Beta Band

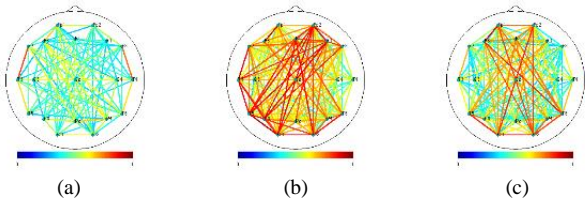


Fig. 9. Head map average connectivity plots for (a) interictal spike (b) spike with slow wave complex (c) repetitive spike and slow wave complex from Beta Band

The patterns extracted from Beta band as shown in Fig. 9 delineated different structures for SSC and RSS from other frequency bands. The average connectivity head map plots show less stronger connections including a weaker propagation. For IS type, the same area of cortex between (F7-T3) and (F8-T4) electrodes still contain the strongest connection indicating a focalized type of epilepsy.

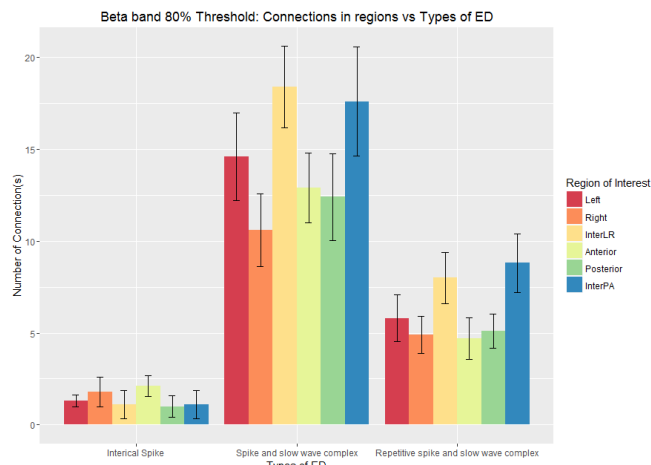


Fig. 10. Mean and standard deviation with 80% threshold in Beta band

The null hypotheses have not been rejected. The IS type provides ($F(5, 54) = 0.453$, p-value > 0.80), SSC type provides ($F(5, 54) = 1.739$, p-value > 0.14) and RSS type provides ($F(5, 54) = 1.985$, p-value > 0.09). In general, the analysis showed that the number of connections in every type of ED is not different across the ROIs.

IV. DISCUSSION

The presented work focused on examining the patterns generated from the extraction of EEG functional connectivity patterns during the occurrence of EDs. With the quantification of the strongest connections presented in each of the frequency bands and in the different ROIs, the characteristics of each type of ED show significance differences that can be used for a classification approved method. A similar approach to the previous analysis [4] was performed on the data, but the functional connectivity extraction was done by using cross-correlation method, which is prone to the error induced by

volume conduction. The same work was performed in [14] and [15] using similar approaches, but without examining the occurrence of EDs in the different frequency bands. It is interesting to apply different generative and discriminative classification approaches to the information selected frequency bands and compare the results for practical applications [16, 17, and 18].

However, the outcome of the connectivity analysis by using coherence has to be interpreted with care. This method does not provide causality assessment, where the flow of information cannot be determined. The aforementioned case leads to the limitation of the interpretation of the results. Even though the origin of certain synchronizations cannot be determined, the actual connections between and within brain regions will help in the assessment and diagnosis of epileptic patients.

V. CONCLUSION

The quantification and extraction of functional connectivity patterns using scalp EEG can generate important features that can be used to classify the type of epilepsy. The patterns extracted by performing coherence analysis revealed different characteristics of each type of EDs exhibited in different frequency bands. Specific patterns of connectivity along the cortex are obtained as a function of the neurological disorder (epilepsy) using coherence analysis. This method measures the consistency of the relative amplitude and phase between a pair of signals, which defines the strength of the connectivity between all pair-wise electrodes. Whether the seizure event will be focalized or generalized type of epilepsy, these distinct features and characteristics of the connectivity maps in each frequency band can be used for classification, which in turn will lead to enhanced diagnosis of the disorder.

ACKNOWLEDGMENT

The study was supported by the National Science Foundation under grants CNS 1532061, CNS-0959985, HRD-0833093, CNS-1042341, CNS-1551221, and IIP-1338922. Support of the Ware Foundation is also greatly appreciated.

REFERENCES

- [1] Fisher, R. S., Boas, W. V. E., Blume, W., Elger, C., Genton, P., Lee, P., & Engel, J. (2005). Epileptic seizures and epilepsy: definitions proposed by the International League Against Epilepsy (ILAE) and the International Bureau for Epilepsy (IBE). *Epilepsia*, 46(4), 470-472.
- [2] van Mierlo, P., Papadopoulou, M., Carrette, E., Boon, P., Vandenberghe, S., Vonck, K., & Marinazzo, D. (2014). Functional brain connectivity from EEG in epilepsy: Seizure prediction and epileptogenic focus localization. *Progress in neurobiology*, 121, 19-35.
- [3] Stam, C. J., Nolte, G., & Daffertshofer, A. (2007). Phase lag index: assessment of functional connectivity from multi channel EEG and MEG with diminished bias from common sources. *Human brain mapping*, 28(11), 1178-1193.
- [4] Janwattanapong, P., Cabrerizo, M., Rajaei, H., Ardila, A., Arias, S. & Adjouadi, M. (2016, December). Epileptogenic brain connectivity patterns using scalp EEG. In GlobalSIP, in press
- [5] S. Sargolzaei , M. Cabrerizo, M. Goryawala, A. Salah Eddin, "Scalp EEG brain functional connectivity networks in pediatric epilepsy", Computers in Biology and Medicine, Vol. 56 pp. 158-166, Jan. 2015.

- [6] S. Sargolzaei, M. Cabrerizo, A. Sargolzaei, S. Noei, H. Rajaei, A. Salah Eddin, A. Pinzon-Ardila, S. M. Gonzalez Arias, P. Jayakar and M. Adjouadi, "A probabilistic approach for pediatric epilepsy diagnosis using brain functional connectivity networks," *BMC Bioinformatics*, Vol. 16, Suppl. 7, April 2015
- [7] Salah Eddin, J. Wang, W. Wu, S. Sargolzaei, B. Bjornson, R. Jones, W.D. Gaillard, and M. Adjouadi, "The effects of pediatric epilepsy on a language connectome", *Human Brain Mapping*, Vol. 35 (12), pp. 5996-6010, December 2014
- [8] Brodie, M. J., & Kwan, P. (2002). Staged approach to epilepsy management. *Neurology*, 58(8 suppl 5), S2-S8.B.
- [9] Nunez, Paul L., et al. "EEG coherency: I: statistics, reference electrode, volume conduction, Laplacians, cortical imaging, and interpretation at multiple scales." *Electroencephalography and clinical neurophysiology* 103.5 (1997): 499-515.
- [10] Adeli, H., Zhou, Z., & Dadmehr, N. (2003). Analysis of EEG records in an epileptic patient using wavelet transform. *Journal of neuroscience methods*, 123(1), 69-87.
- [11] Nunez PL, Srinivasan R. Electric fields of the brain: the neurophysics of EEG. 2nd ed. New York: Oxford University Press; 2006a.
- [12] Delorme, A., & Makeig, S. (2004). EEGLAB: an open source toolbox for analysis of single-trial EEG dynamics including independent component analysis. *Journal of neuroscience methods*, 134(1), 9-21.
- [13] Welch PD. The use of fast Fourier transform for the estimation of power spectra: a method based on time averaging over short, modified periodograms. *IEEE T Audio Electroacoust* 1967;AU-15:70-3.
- [14] Shafi, M. M., Westover, M. B., Oberman, L., Cash, S. S., & Pascual-Leone, A. (2014). Modulation of EEG functional connectivity networks in subjects undergoing repetitive transcranial magnetic stimulation. *Brain topography*, 27(1), 172-191.
- [15] Dodel, S., Herrmann, J. M., & Geisel, T. (2002). Functional connectivity by cross-correlation clustering. *Neurocomputing*, 44, 1065-1070
- [16] H. Su, S. Tian, Y. Cai, Y. Sheng, C. Chen and M. Najafian, "Optimized extreme learning machine for urban land cover classification using hyperspectral imagery" in *Frontiers of Earth Science (FESCI) 2016*, Springer, pp. 1-8.
- [17] R. Nabie, M. Najafian, M. Parekh, P. Jancovic, and M. Russell, "Delay reduction in real-time recognition of human activity for stroke rehabilitation," in *SPLINE*, pp. 70-74, 2016.
- [18] M. Liu, H. Liu, C. Chen and M. Najafian, "Energy-based global ternary image for action recognition using sole depth sequences," *3D Vision*, pp. 1-9, 2016